Proceedings 10th NUMGE 2023
10th European Conference on Numerical Methods in Geotechnical Engineering
Zdravkovic L, Kontoe S, Taborda DMG, Tsiampousi A (eds)

https://doi.org/10.53243/NUMGE2023-59

Egg-shaped large cantilever excavation pit using Plaxis 3D

P. Schauber[1] , J. Sarath Chandra Prasad[1]

[1]*Keller Grundbau Gmbh*

ABSTRACT: In general, cylindrical excavation pits are designed using Finite Element (FE) axisymmetric models. However, these models are not anymore valid for constructing elliptical shaped excavation pits as they consist of different wall radii generating different hoop stresses and therefore only 3D analysis shall be considered. This paper presents a project of merging two cylindrical deep excavation pits into a single "egg - shape" cantilever excavation pit using Plaxis 3D. The paper details appropriate Plaxis model, soil and wall parameters, and all the other important aspects those were considered into the calculation results and design aspects.

Keywords: Egg shape excavation, Deep Excavation support system, Plaxis 3D

1 INTRODUCTION

The expansion of TUBLI Sewage Treatment Plant (STP) -Phase 4 in Kingdom of Bahrain aims to upgrade the secondary treatment unit using the 'HYBACS' technique, which is to improve the quality of water and increased flow of waste water, taking the average daily flow capacity of 200,000 m3/day to reach a full average daily flow capacity of 400,000 m3/day.

The project deploys proprietary SMARTTM reactor units that stimulate a special and specific bacterial pattern with a high biological activity that has the ability to deal with different levels of organic materials. This will reflect on the quality of waters discarded in Tubli Bay.

The project includes a collection room for the wastewater streams that flow at a level of 21m under the ground and an inlet pumping station at a level of 25.1m under the ground that will receive wastewater from the collection room. For the construction of inlet pumping station at a higher depth and considering the complexities in its geometry, an egg-shaped secant pile wall excavation support system was proposed and discussed in this paper.

2 GEOMETRY OF EXCAVATION AND RETAINING WALL CHARACTERISTICS

2.1 Excavation's geometry

The two pits have a corresponding diameter of Ø29.20m and Ø14.40m. Figure 1 illustrates secant pile wall formed with three different radii of curvature in order to contain the two pits in one.

The radii of curvature for the three sections are as follows,

- Section 1: Ø15.3m (Radius: 7.65m)
- Section 2: Ø60.6m (Radius: 30.30m)
- Section 3: Ø30.1m (Radius: 15.05m)

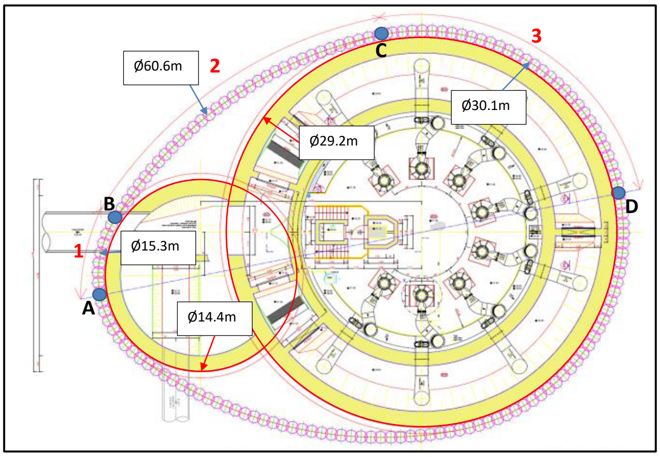

Figure 1. Layout drawing of the secant pile wall and Inlet Pumping Station

The excavation depth is 25.1m.

2.2 Retaining wall characteristics

2.2.1 Piles

- Piles geometry and overlap

A total number of 156 piles with a diameter of Ø900mm and center to center spacing of 700mm is considered. As shown on the figure 2, the overlap thickness is about 566mm without considering deviation.

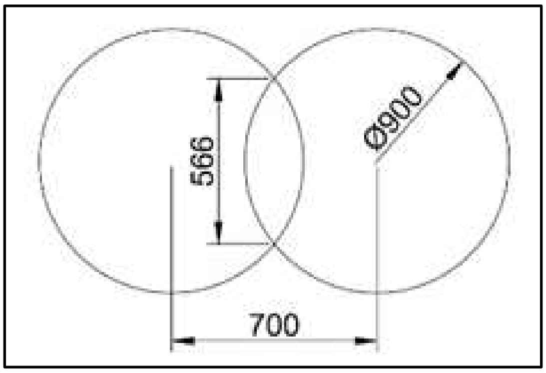

Figure 2. Overlap thickness considered in the design

- Drilling tool

The piles are installed from natural ground level to 28m depth using cased bored piles system, with a temporary casing installed for full depth of pile penetrating into deep rock layers.

This system permits piles to install with tight verticality tolerances and resulting deviation is negligible. For this secant pile wall, the maximum measured deviation is less than 0.25%. Therefore, the overlap thickness of 566mm is considered into the design assumptions on the whole secant pile wall height.

Only the secondary piles are reinforced, which means that only half of the piles are reinforced.

2.2.2 *Caping beam*

A caping beam of 1.0mx1.0m is installed on top of the secant pile wall.

During excavation, a smaller intermediate ring beam of 0.6mx0.6m is installed at an elevation +40.50m.

2.2.3 *Secant pile wall cross-section*

Figure 3 shows the secant pile wall cross-section:

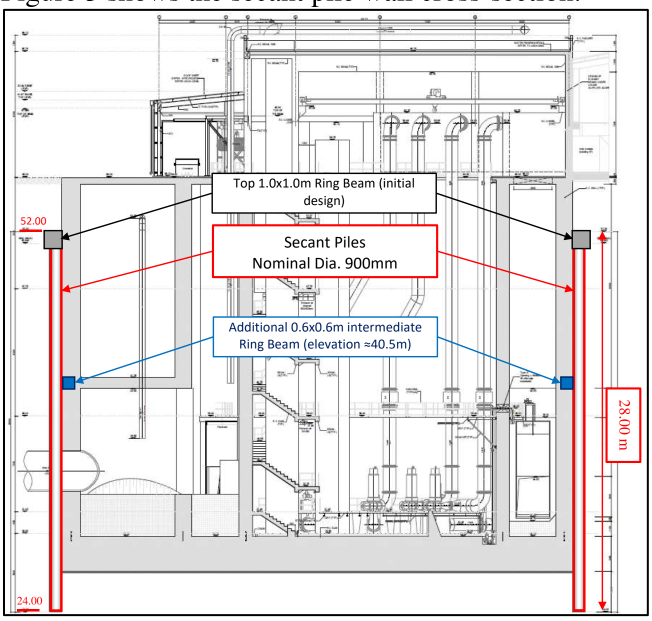

Figure 3. Section drawing of the secant pile wall and Inlet Pumping Station

3 DESIGN CRITERIA

Since no design criteria specific to the project was given, Keller has set a design criterion for secant piling works as listed:

- Maximum allowable wall deflection in horizontal direction = 20mm
- Maximum heave/ settlement around the excavation pit = ±25mm
- Overall factor of safety on uplift = 1.39

In addition to the above-mentioned criteria, the structural integrity of the wall has been checked. The wall had to be designed considering a maximum crack opening, defined as per French national annex of the Eurocode: NF P 94-262 §6.4.2 as specified:

- $\sigma_s < 1000\ w_{max}$ for bent elements;
- $\sigma_s < 600\ w_{max}$ for completely outstretched elements.

Where σ_s is the maximal stress value allowable in the reinforcement bar next to the crack and w_{max} the calculated opening of the cracks.

According to the application guide to the EN 1992.1.1 (2004), the cracks opening w_{max} shall be limited to the following values:

Table 1. Table 7.1N of EN1992.1.1 (2004)

Exposure Class	Reinforced members and prestressed members with unbonded tendons	Prestressed members with bonded tendons
	Quasi-permanent load combination	Frequent load combination
XC0, XC1	0.4[1]	0.2
XC2, XC3, XC4	0.3	0.2[2]
XD1, XD2, XD3, XS1, XS2, XS3		Decompression

Note 1: For X0, XC1 exposure classes, crack width has no influence on durability and this limit is set to give generally acceptable appearance. In the absence of appearance conditions this limit may be relaxed.
Note 2: For these expose classes, in addition, decompression should be checked under the quasi-permanent combination of loads.

That is to say an allowable stress of 300 MPa (1000 * 0.30mm) for the retaining wall piles for long term situation and concrete exposure class of XS2.

From the calculations, it was clear that the crack opening for relevant long-term and SLS quasi-permanent condition was the most severe case and ULS calculation checking are not detailed in this article.

4 GEOTECHNICAL PROFILE

The geotechnical profile can be describer in three parts:

- Upper soil up to 8m depth
- Weathered rock up to 10m depth
- Intact rock from 10 to 35m depth

4.1 *Upper soil*

The upper part of the geotechnical profile is mainly composed of dense to very dense sand showing cone penetration value q_c from 10 to 30 MPa.

4.2 *Rock formation*

The rock formation is composed of intact limestone with RQD values varying from 20 to 90% across the rock formation, except the layer below 31m depth showing RQD of 0%. The unconfined compressive strength (UCS) is quite homogeneous with an average value of 5MPa for the top 14m, and 15MPa for the bottom part.

4.3 *Water table*

4.3.1 *Shallow water*

A shallow water table was observed at 2 m depth from existing ground level and was measured via wells.

4.3.2 *Deep aquifer*

Bahrain Island is known to be installed on top of a deep aquifer called Alat aquifer. The figure 4 below shows that the depth of the aquifer varies across the island.

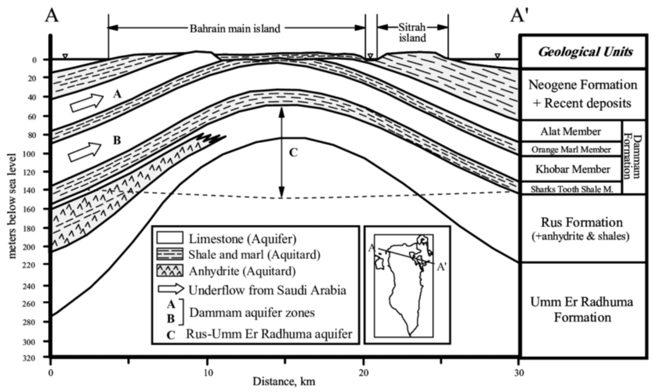

Figure 4. Illustration of Alat aquifer, Zubari, WK. (2005)

Based on the RQD of 0% below 31m depth, it was initially assumed that this may represent the top of the aquifer. This was confirmed during excavation which means that the top of aquifer was at a maximum depth of 3m below the bottom of the piles and 5.9m below bottom of excavation.

4.3.3 *Permeability*

Some Lugeon tests were performed into the limestone rock and were showing permeability from $1x10^{-6}$ m/s and $1x10^{-5}$ m/s. The measured permeability is relatively high that may be explained by water easily flowing through rock fractures.

4.3.4 *Water drawdown*

The natural ground water table is about 2m in depth.

In order to reduce the water pressure on the wall, a general water draw down outside wall periphery was realized with seven wells installed outside the wall and at an approximate distance of 5m.

Seven wells that were installed initially, were not showing any relevant water drawdown despite pumping water hugely. It was assumed that the wells were drilled too deeply, probably pumping water from Alat aquifer and seven additional shorter wells were carried out.

An average water drawn down from 50m to 40m in elevation were measured. But with regard to the difficulty to reduce the water pressure, the design was made considering only water pumped from inside excavation, leading to an outside water table at 46m in elevation. Because of additional pore water pressure acting on the wall, an additional intermediate ring beam were requested as shown on figure 3.

5 CALCULATION MODEL IN PLAXIS

The calculations are carried out with Plaxis 3D.

5.1 *Geometry and structural elements*

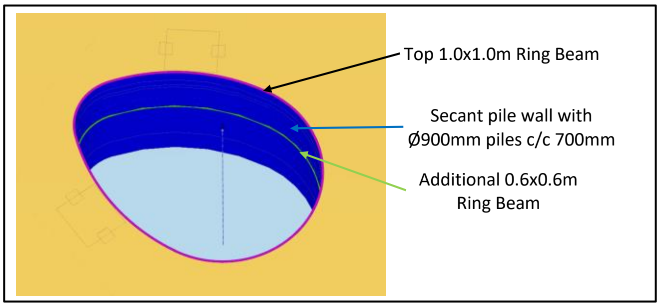

Figure 5. Plaxis 3D model

The secant pile wall was modelled with plate element. The flexural rigidity EI is non-isotropic in order to take into account wall inertia between vertical and horizontal behaviour with:

- Horizontal inertia $I = \frac{bh^3}{12} = \frac{1*0.566^3}{12} = 0.01511m^4$
- Vertical inertia: $I = \frac{bh^3}{12} = \frac{1*0.83^3}{12} = 0.04765m^4$

The ratio between vertical and horizontal inertia is about 3.

During excavation phase, a transitory deformation modulus of E = 20 GPa is considered.

For the last excavation phase, the deformation modulus considered is relevant to long-term case situation considering cracked concrete. The relevant deformation modulus, E = 10 GPa.

5.2 *Soil and rock input properties*

The soil is modelled with either Hardening Soil (HSM) or Hardening Soil Small strain (HSsmall) constitutive models. The rock layer is modelled with Hoek-Brown constitutive model following sensitivity analysis comparing with HSsmall. The following table summarize the soil input parameters:

Table 2. Soil input parameters

Parameters		Units	Soil layers				
			Very dense sand	**Calcarenite**	**Organic material**	**Very dense sand 2**	**Weathered limestone**
			From 52.0 to 49.5 m	From 49.5 to 48.0 m	From 48.0 to 47.2 m	From 47.2 to 44.0 m	From 44.0 to 42.0 m
General	Material Model	[-]	Hardening soil	HS small	Hardening soil	HS small	HS small
	γ_{unsat}	[kN/m^3]	18	19	15	19	21
	γ_{sat}	[kN/m^3]	20.5	21.5	16	21.5	21
Stiffness (HSM)	E_{50}^{ref}	[MPa]	40.0	100.0	1.25	60.0	60.0
	E_{oed}^{ref}	[MPa]	40.0	100.0	1.25	60.0	60.0
	E_{ur}^{ref}	[MPa]	120.0	300.0	3.75	180.0	180.0
	power (m)	[-]	0.5	0.7	1.0	0.5	0.7
	$p^{ref} = \sigma'_1$	[kPa]	20	42	52	73	104
Strength	C'_{ref}	[kPa]	0	20	0.5	0	5
	ϕ'	[°]	40	35	20	38	32
	Ψ	[°]	10	5	-	8	2
Permeability	k_x	[m/s]	1.00E-05	1.00E-06	1.00E-08	1.00E-05	1.00E-05
	k_y	[m/s]	1.00E-05	1.00E-06	1.00E-08	1.00E-05	1.00E-05

From 42.0m to 22.0m elevation, the rock is modelled using Hoek-Brown constitutive modelled as detailed in the Table 3:

Table 3. Rock input parameters using Hoek-Brown

Rock layers			**Limestone 1**	**Limestone 2**	**Limestone 3**	**Limestone 4**
			From +42.0 to +35.0m	From +35.0 to +26.0m	From +26.0 to +21.0m	From +21.0 to +16.0m
RQD	Average RQD estimation	[%]	30	60	20	5
E	Young's modulus	[kPa]	600,000	600,000	800,000	600,000
ν	Poisson's ratio	[-]	0.3	0.3	0.3	0.3
σ_{ci}	Uni-axial compressive strength of the intact rock	[kPa]	6,000	6,000	15,000	6,000
mi	Intact rock parameter	[-]	10	12	8	7
GSI	Geological Strength Index	[-]	50	70	45	35
D	Disturbance factor	[-]	0	0	0	0
ψ_{max}	Dilatancy angle (at $\sigma'3 = 0$)	[-]	0	0	0	0
σ_ψ	Absolute value of confining pressure	[kPa]	0	0	0	0

A sensitivity analysis was carried out: modelling the rock using HSsmall constitutive model after having fitted the Morh-Coulomb strength parameters as stated by Hoek et al. (2002). The results were in the same order of magnitude showing that the results are not sensitive to the constitutive model.

6 CALCULATION RESULTS

6.1 Displacement

Figure 6 shows the wall displacement at the end of excavation:

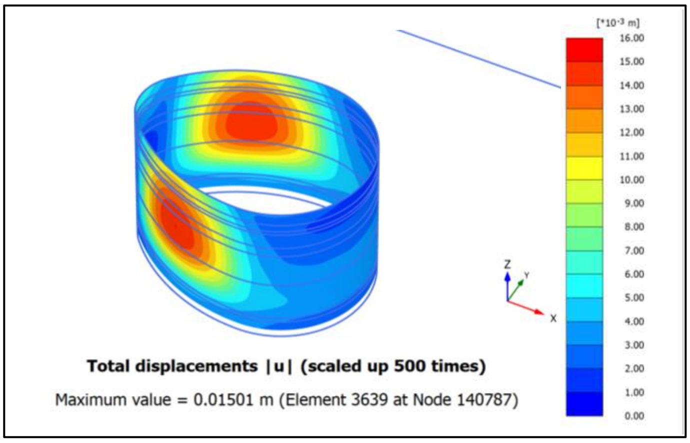

Figure 6. Wall displacement at end of excavation

The displacement of the secant pile wall is low and about 1.5cm. It can be seen that the maximum displacement is located where the wall radius of curvature is the highest (Section 2).

Figure 7 illustrates amplified the deformed shape of the secant pile wall.

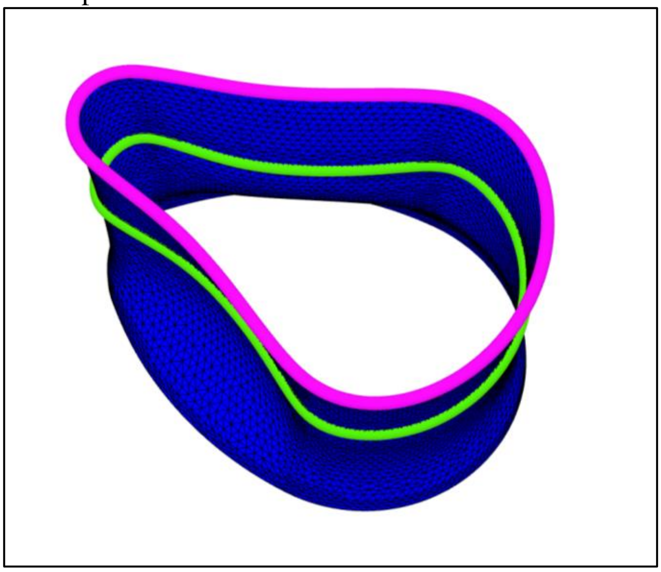

Figure 7. Deformed mesh of the wall (scale 500 times)

6.2 Efforts in the wall

The loads into the secant pile wall were checked, mainly focusing on the bending moment in both directions: vertical and horizontal. Vertical bending was checked in order to design the steel rebar cage of the piles when the horizontal bending was checked in order to guarantee the structural connection integrity between the secant piles. The latter is mandatory to ensure that the connection between piles remain complete which means that hoop forces remain fully operational.

6.2.1 Vertical bending

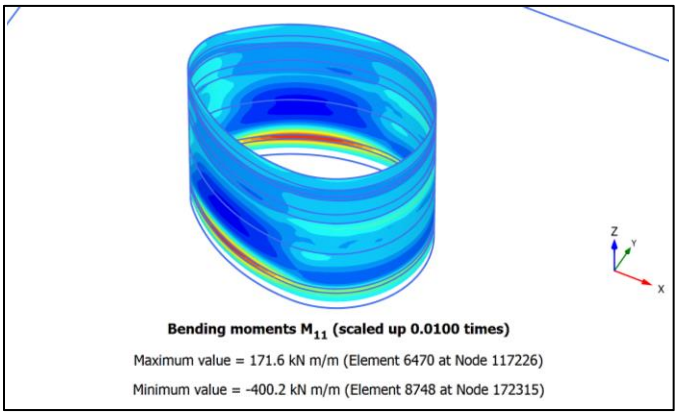

Figure 7. Vertical bending moment

The vertical bending moment is up to 400kN.m/m and maximum values are located at the bottom of excavation. It can be noticed that the part of the wall with higher radius of curvature is showing higher variation of bending moment.

The vertical bending moment was taken by the secondary piles which are reinforced with 9 bars Ø25mm on the entire length. Additional 9 bars of Ø25mm were used to strengthen the bottom 8m of the piles.

6.2.2 Horizontal bending

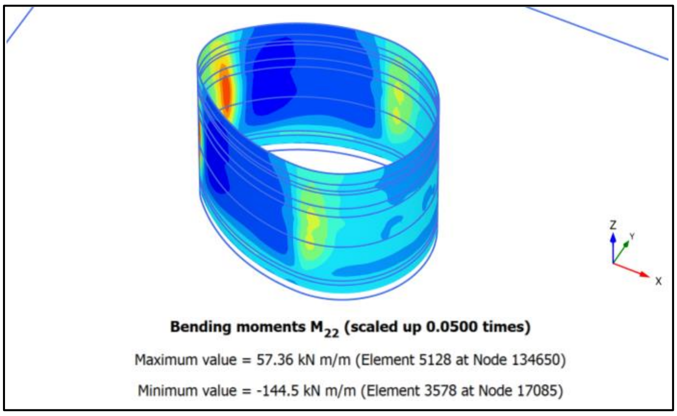

Figure 8. Horizontal bending moment

The horizontal bending is fairly low but higher values are located when there is a variation of the radius of curvature of the secant pile wall. And the higher is the difference of radius of curvature, the higher is the bending moment.

The hoop compression is then extracted in order to check that the load eccentricity within the secant pile overlap is allowable.

6.2.3 Hoop compression

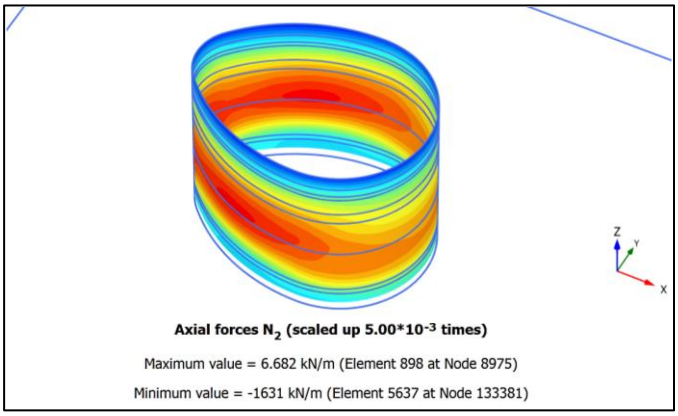

Figure 9. Hoop compression

The hoop force reduces with the increase of radius of curvature, which means that the arching mechanism within the soil/rock layer is less efficient. It leads to higher active earth pressure and which is also confirmed by higher wall displacement.

The horizontal load eccentricity (horizontal bending/hoop force) is calculated at different elevations. The wall depth within the soil layers and for smaller radius of curvature is showing a load eccentricity close to central nucleus edge. The following figure 10 show the load eccentricity at +49m in elevation:

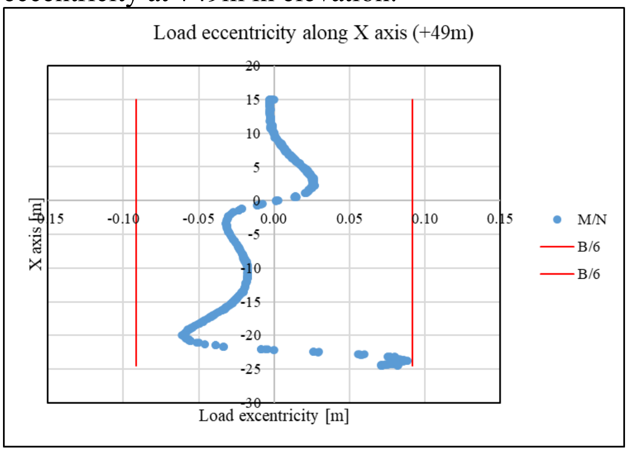

Figure 10. Horizontal load eccentricity at +49m elev.

The load eccentricity is very close to the central nucleus edge (=566/6 = 94mm)

In order to stay in a conservative case, the top 10m of the wall in section 1 (Ø15.3m) is modified with reduced horizontal inertia by a factor of 3. This leads to higher loads transferred to the ring beams and additional steel reinforcement were considered.

6.3 Conclusion on calculation results

As expected, the larger is the radius of curvature of the secant pile wall, the less arching effect applies, and the more vertical bending moment appears. This part of the wall is also showing the highest displacement which remains quite low and in the range of 1.5cm.

The horizontal bending moment can be critical at some points and especially when the radius of curvature varies. The higher the radius of curvature varies, the more critical is the resulting load eccentricity. The ring beams are taking some part of the bending in order to maintain the hoop forces required for the global hoop compression and global behaviour of the wall.

7 MICROTUNNELLING

The excavation pit will be connected to an adjacent pit called collection chamber and separated from about 400 meters. The opening through the secant pile wall will be carried out with a Micro tunnelling from a diameter of Ø3.2m at a depth of 17.6m.

Because rebar cages composed of glass fibres are not easy to get in Bahrain, the piles crossed by the micro tunnelling are made of polymer fibres concrete, including steel rebar cage on top and bottom. Three piles had to be modified as detailed in figure 11.

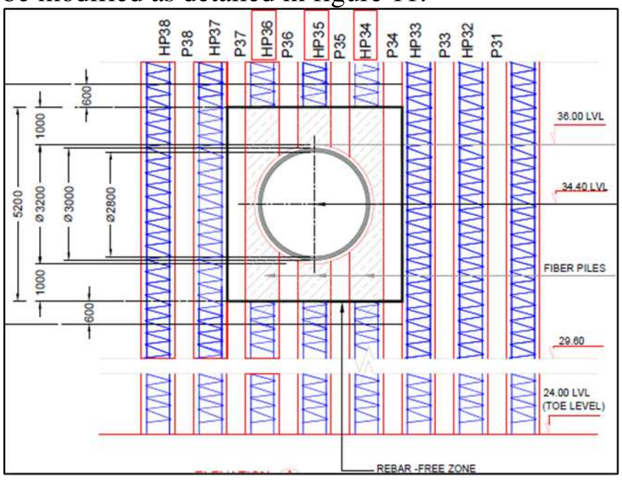

Figure 11. Secant pile wall adjustment for micro tunnelling entry

In any part of this 5.2mx4.9m area has been checked focusing on horizontal and vertical load eccentricity. The whole area was showing fully compressed piles in both vertical and horizontal directions, which confirm that fibre reinforced concrete would be sufficient to maintain pile integrity.

8 MONITORING

Some monitoring of the secant pile wall displacement was realized both by Keller and by the client for a during more than a year. The maximum wall displacement measured is in the range of 7-8mm. Unfortunately, the displacements are generally so low that it is difficult to make any interpretation of it. It can be concluded that the design and calculation carried out with Plaxis 3D are on the conservative side.

9 CONCLUSION

Merging two pits into one larger secant pile wall is an efficient way to simplify many steps during excavation and structural works.

Nevertheless, it requires advanced design capabilities like soil and wall interaction with 3D Finite Element Method (FEM). This method is the only solution that considers many aspects of the design like various different arching mechanism leading to heterogeneous secant pile wall reaction depending on radius of curvature. It also gives the possibilities to check the internal wall forces at any location and especially the resulting horizontal load eccentricity when the radius of curvature of the wall changes.

The external water draw down was a good solution to reduce the water pressure on the wall but technically tedious. Therefore, an additional intermediate ring beam was installed in order to increase the global factor of safety.

The monitoring was showing less than half of the calculated wall displacement. This shows that the Plaxis 3D calculation was carried out on the conservative side, at least confirmed by the water table considered not as low as measured during dewatering.

It is also to be noticed that installing Ø900mm pile at 28m depth at 700mm c/c with sufficient pile overlap is only possible thanks to drilling technic of the pile: the cased bored pile was showing a maximum deviation of 0.3%.

Steel pile reinforced were locally replaced by polymer fibres for allowing the micro tunnelling of Ø3.2m to pass.

Figure 12. Secant pile wall after completion of excavation

10 REFERENCES

EN1992-1-1 (2004): Eurocode 2: Design of concrete structures - Part 1-1 : General rules and rules for buildings

Zubari, WK., 2005, Spatial and temporal trends in groundwater resources in Bahrain, *Emirates Journal for Engineering Research, 10(1), 57-67 (2005)*

Hoek, E., Carranza-Torres, C., Corkum, B., 2002, Hoek-Brown failure criterion, *Proc. NARMS-TAC Conference, Toronto*, 2002, 1, 267-273

Hoek, E., Brown, E.T., 2018, The Hoek-Brown failure criterion and GSI, *Journal of Rock Mechanics and Geotechnical Engineering (2018)*

Plaxis 3D Manual, 2022.